A

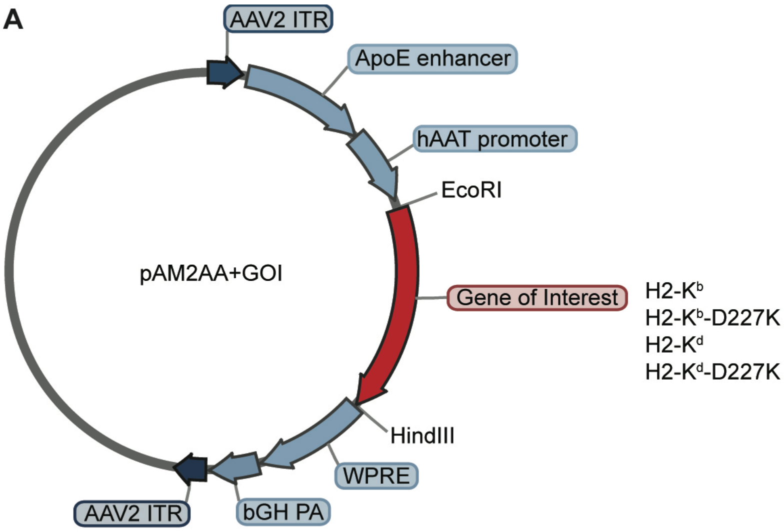

Supplementary Figure 1. Features of AAV vectors encoding MHC class I molecules. (**A**) Constructs encoding AAV2 inverted terminal repeats (ITRs), genes of interest and regulatory elements were packaged into an AAV8 capsid (AAV2/8 vector). ApoE = apolipoprotein E, hAAT = human alpha-1 antitrypsin, WPRE = woodchuck hepatitis virus post-transcriptional regulatory element, bGH PA = bovine growth hormone polyadenylation signal. (**B** and **C**) Alignment of K^b or K^d sequences showing the aspartic acid (D) to lysine (K) mutation at position 227.

B

```
H2-Kb         GPHSLRYFVTAVSRPGLGEPRYMEVGYVDDTEFVRFDSDAENPRYEPRARWMEQEGPEYWERETQKAKGNEQSFRVDLRT  80
H2-KbD227K    GPHSLRYFVTAVSRPGLGEPRYMEVGYVDDTEFVRFDSDAENPRYEPRARWMEQEGPEYWERETQKAKGNEQSFRVDLRT  80

H2-Kb         LLGYYNQSKGGSHTIQVISGCEVGSDGRLLRGYQQYAYDGCDYIALNEDLKTWTAADMAALITKHKWEQAGEAERLRAYL  160
H2-KbD227K    LLGYYNQSKGGSHTIQVISGCEVGSDGRLLRGYQQYAYDGCDYIALNEDLKTWTAADMAALITKHKWEQAGEAERLRAYL  160

H2-Kb         EGTCVEWLRRYLKNGNATLLRTDSPKAHVTHHSRPEDKVTLRCWALGFYPADITLTWQLNGEELIQDMELVETRPAGDGT  240
H2-KbD227K    EGTCVEWLRRYLKNGNATLLRTDSPKAHVTHHSRPEDKVTLRCWALGFYPADITLTWQLNGEELIQKMELVETRPAGDGT  240

H2-Kb         FQKWASVVVPLGKEQYYTCHVYHQGLPEPLTLRWEPPPSTVSNMATVAVLVVLGAAIVTGAVVAFVMKMRRRNTGGKGGD  320
H2-KbD227K    FQKWASVVVPLGKEQYYTCHVYHQGLPEPLTLRWEPPPSTVSNMATVAVLVVLGAAIVTGAVVAFVMKMRRRNTGGKGGD  320

H2-Kb         YALAPGSQTSDLSLPDCKVMVHDPHSLA 348
H2-KbD227K    YALAPGSQTSDLSLPDCKVMVHDPHSLA 348
```

C

```
H2-Kd         GPHSLRYFVTAVSRPGLGEPRFIAVGYVDDTQFVRFDSDADNPRFEPRAPWMEQEGPEYWEEQTQRAKSDEQWFRVSLRT  80
H2-KdD227K    GPHSLRYFVTAVSRPGLGEPRFIAVGYVDDTQFVRFDSDADNPRFEPRAPWMEQEGPEYWEEQTQRAKSDEQWFRVSLRT  80

H2-Kd         AQRYYNQSKGGSHTFQRMFGCDVGSDWRLLRGYQQFAYDGRDYIALNEDLKTWTAADTAALITRRKWEQAGDAEYYRAYL  160
H2-KdD227K    AQRYYNQSKGGSHTFQRMFGCDVGSDWRLLRGYQQFAYDGRDYIALNEDLKTWTAADTAALITRRKWEQAGDAEYYRAYL  160

H2-Kd         EGECVEWLRRYLELGNETLLRTDSPKAHVTYHPRSQVDVTLRCWALGFYPADITLTWQLNGEDLTQDMELVETRPAGDGT  240
H2-KdD227K    EGECVEWLRRYLELGNETLLRTDSPKAHVTYHPRSQVDVTLRCWALGFYPADITLTWQLNGEDLTQKMELVETRPAGDGT  240

H2-Kd         FQKWAAVVVPLGKEQNYTCHVHHKGLPEPLTLRWKLPPSTVSNTVIIAVLVVLGAAIVTGAVVAFVMKMRRNTGGKGVNY  320
H2-KdD227K    FQKWAAVVVPLGKEQNYTCHVHHKGLPEPLTLRWKLPPSTVSNTVIIAVLVVLGAAIVTGAVVAFVMKMRRNTGGKGVNY  320

H2-Kd         ALAPGSQTSDLSLPDGKVMVHDPHSLA  347
H2-KdD227K    ALAPGSQTSDLSLPDGKVMVHDPHSLA  347
```

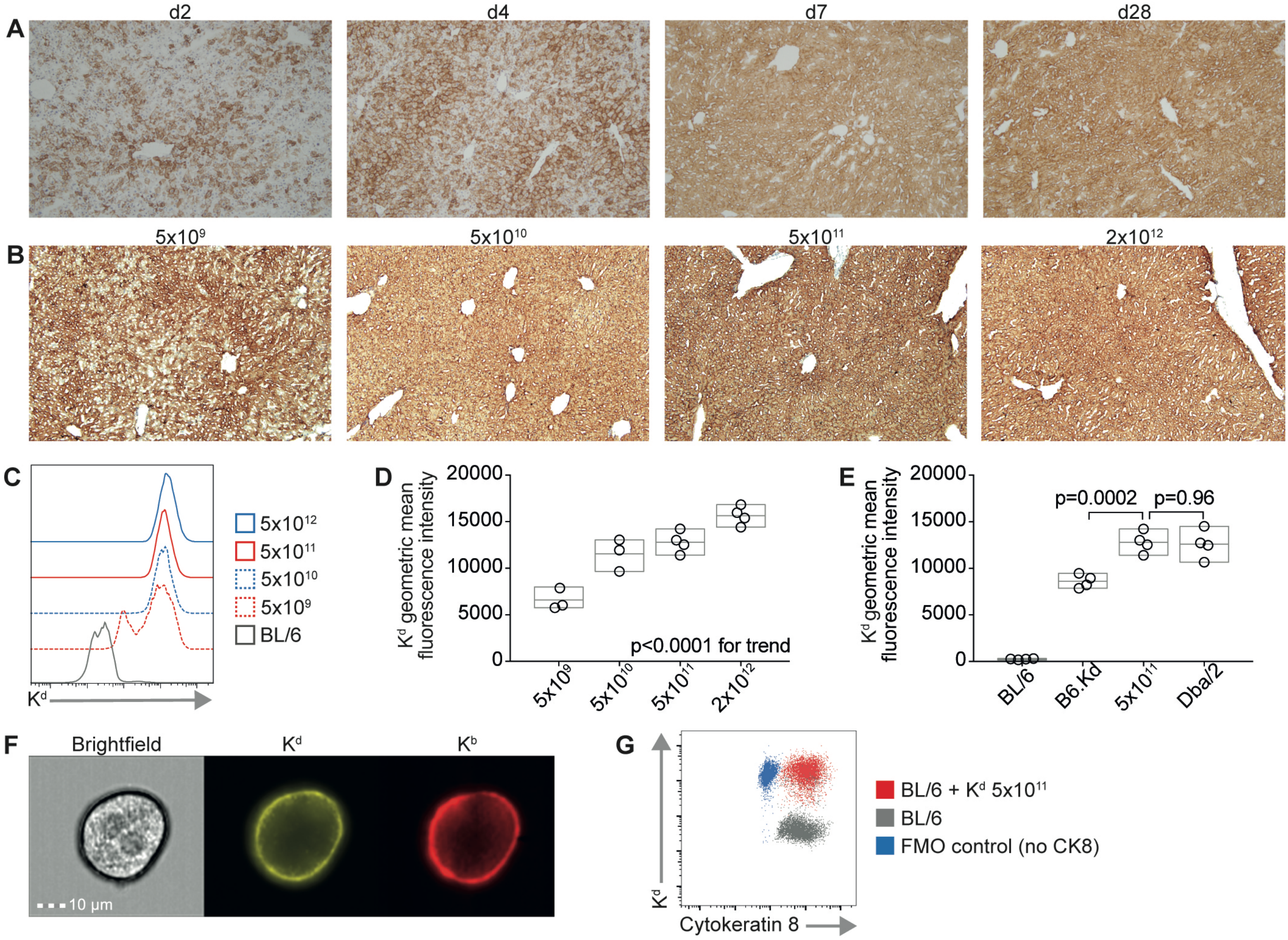

Supplementary Figure 2. In vivo expression of K^d in livers of mice transduced with AAV-K^d. (**A**) C57BL/6 mice (n=3/group) were inoculated with 5×10^{11} vgc AAV-K^d. Livers were collected at intervals from 2-28 days post-injection, and frozen sections were stained for K^d expression. Strong expression of K^d in hepatocytes was noted from d2 onwards, and was near-maximal by d7. Representative images are shown. Magnification=200x. The extent of K^d expression on C57BL/6 hepatocytes at d7 following transduction with AAV-K^d at doses ranging from 5×10^{9} to 2×10^{12} vgc was assessed using immunostaining of liver sections (200x) (**B**) and flow cytometry on isolated hepatocytes (**C-D**). 100% of hepatocytes expressed H-2K^d at doses of 5×10^{10} and above, with a trend towards increasing intensity of K^d surface expression as the vector dose was raised (n=3, $p<0.0001$, statistical analysis by one-way ANOVA with post-test for linear trend). At a vector dose of 5×10^{11} vgc AAV-K^d, surface expression of K^d on transduced C57BL/6 hepatocytes was equivalent to the expression of native K^d on hepatocytes of the d-haplotype mouse strain Dba/2, and was greater than the expression of K^d on hepatocytes from the transgenic B6.Kd donor strain (**E**). In panels **D-E**, boxes show min to max, with a line at the mean, n=3-4/group. Isolated hepatocytes from C57BL/6 mice transduced with AAV-K^b were examined by imaging flow cytometry using the AMNIS Imagestream. Transduced cells show typical hepatocyte morphology on the brightfield image, and express both the native MHC class I H-2K^b and the H-2K^d transgene product (**F**). Moreover, isolated transduced cells stain positive for the hepatocyte marker cytokeratin-8 (**G**). A fluorescence minus one (FMO) control, where cytokeratin-8 staining was omitted, is also shown in this panel.

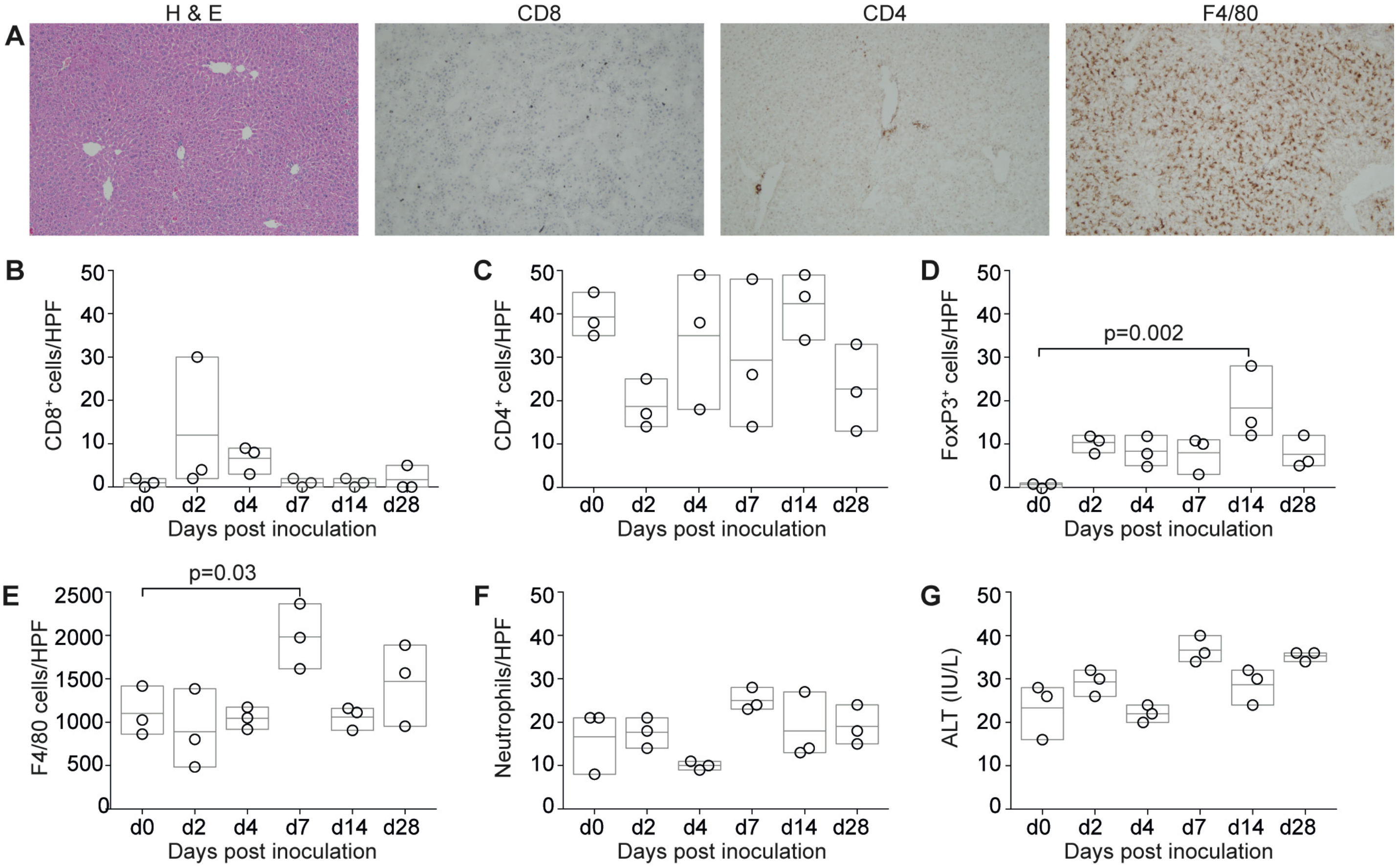

Supplementary Figure 3. Inoculation of C57BL/6 mice with AAV-K^d does not result in liver inflammation. Liver sections from mice transduced with 5x10^{11} vgc AAV-K^d were stained with Haematoxylin and Eosin, and with antibodies against various leucocyte markers (**A**-**F**, supplementary table 1). Liver morphology was normal in transduced mice (**A**). Only small numbers of infiltrating CD8$^+$ T cells (**B**), CD4$^+$ T cells (**C**), and Ly6B.2$^+$ neutrophils (**F**) were detected by immunostaining. The number of FoxP3$^+$ T cells increased from 0.7±0.3 cells/HPF in normal C57BL/6 mice to 18.3±4.9 cells/HPF at d14 after vector inoculation, p=0.002. F4/80-expressing Kupffer cells are plentiful in the livers of normal C57BL/6 mice (1102±165 cells/HPF), and greater numbers of F4/80 expressing cells were observed on d7 post-transduction (1985±216 cells/HPF, p=0.03). Alanine aminotransferase levels in serum (**G**) remained within the normal range for C57BL/6 mice. (n=3/group for all panels **B**-**G**, representative images are shown in **A**, magnification=200x. Boxes in **B**-**G** show min to max, with a line at the mean. Data are given as mean±SEM. Statistical analysis employed one-way ANOVA, followed by Dunnett's multiple comparisons test.

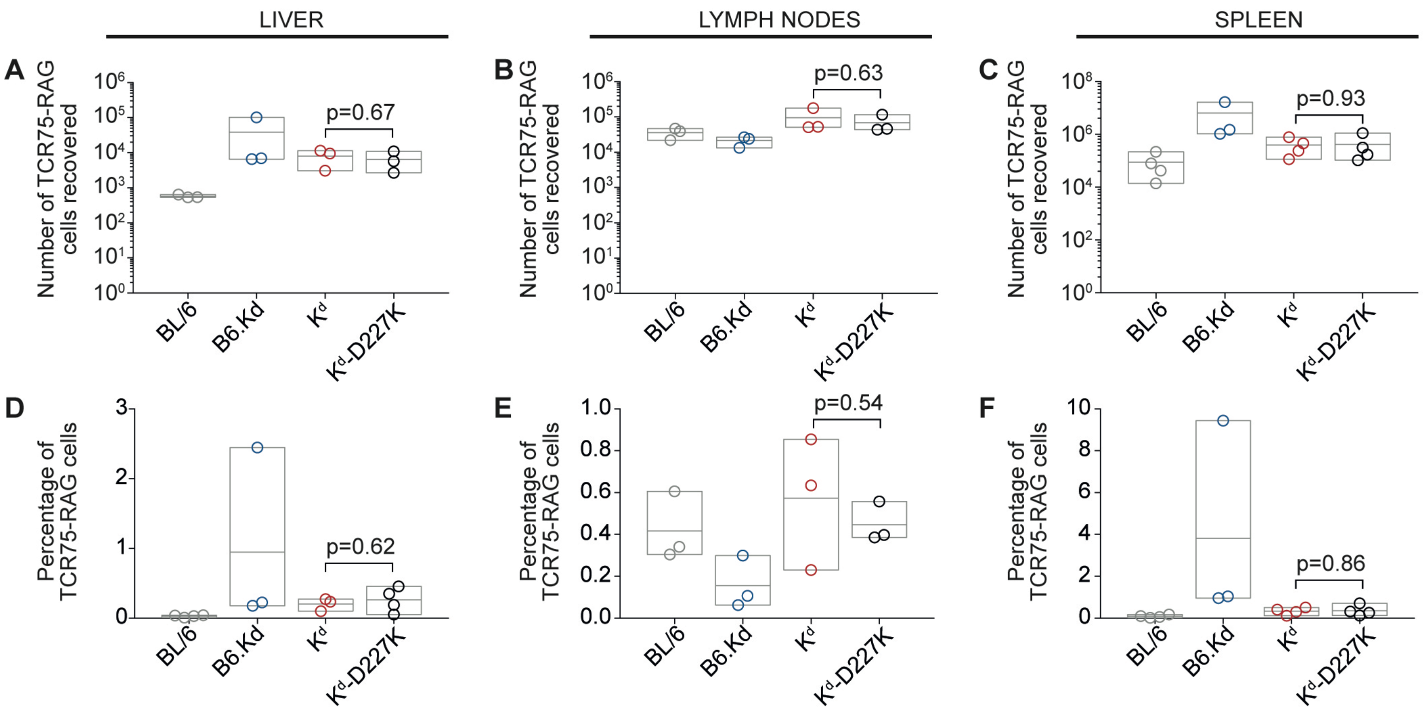

Supplementary Figure 4. Recovery of adoptively-transferred TCR75-RAG T cells from mice inoculated with AAV-K^d or K^d-D227K. (**A**) Very few TCR75-RAG T cells (572±35, identified by co-expression of CD4 and the congenic marker CD45.1) could be recovered from the liver of control C57BL/6 mice at 72 hours following adoptive transfer. In contrast, >6000 CD4$^+$CD45.1$^+$ cells were recovered from the livers of B6.Kd mice or those of C57BL/6 mice inoculated with either AAV-K^d or K^d-D227K. There was no significant difference between recovery of transferred cells from mice in the K^d and K^d-D227K groups (8020±2540 v/s 6413±2380, p=0.67). (**B**) Recovery of transferred TCR75-RAG T cells from the draining LN did not differ between mice transduced with K^d or K^d-D227K vectors (94743±42373 v/s 69223±23987, p=0.63), similarly 3.96x10^5±1.46x10^5 TCR75-RAG cells were recovered from spleens of the K^d group (**C**), compared with 4.22x10^5±2.29x10^5 from spleens of the K^d-D227K-expressing mice (p=0.93). As for the absolute numbers, the proportion of TCR75-RAG cells (expressed as the percentage of all live leucocytes) present in each organ did not differ between mice treated with AAV-K^d and K^d-D227K. In the liver, TCR75-RAG cells comprised 0.20±0.05% of leucocytes in K^d-expressing mice, compared with 0.26±0.09% in mice transduced with AAV-K^d-D227K, p=0.62. In draining LN, these proportions were 0.57±0.18% compared with 0.44±0.06%, p=0.54, and in spleen, TCR75-RAG cells formed 0.33±0.08% of leucocytes from AAV-K^d-treated mice v/s 0.36±0.13%, p=0.86, in the K^d-D227K group. n=3-4 per group, boxes show min to max, with a line at the mean. Recovery of TCR75-RAG cells from mice treated with either AAV-K^d or AAV-K^d-D227K was compared using unpaired T-tests. Data are described as mean±SEM.

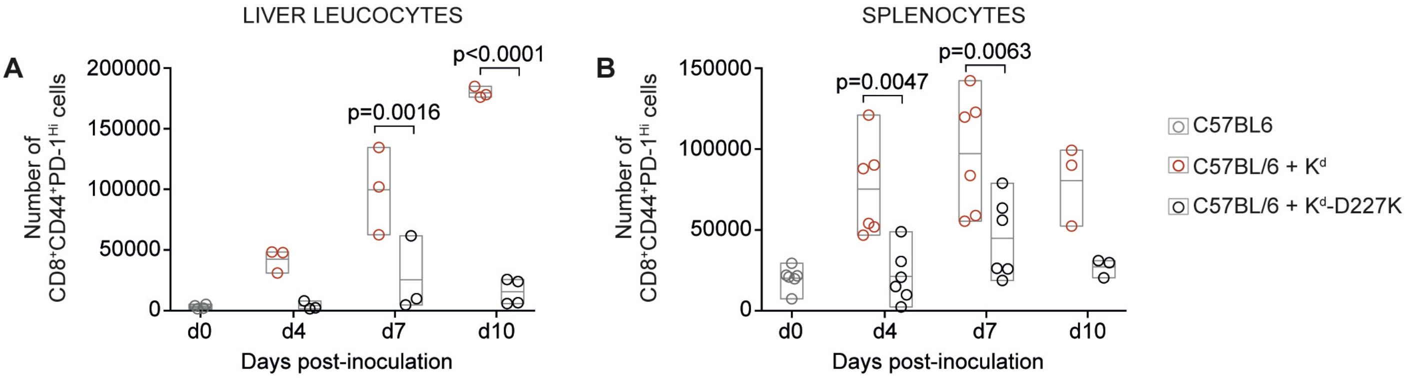

Supplementary Figure 5. Increased numbers of activated $CD8^+$T cells are present in liver and spleen following inoculation with AAV-K^d. $CD8^+$ T cells were isolated from liver and spleen at intervals ranging between 4 and 10 days following inoculation of C57BL/6 mice with AAV-K^d or K^d-D227K. (**A**) The number of activated $CD8^+$ T cells ($CD44^+$PD-1^{Hi}) in the liver peaked on d10 after injection with AAV-K^d. There were significantly more activated $CD8^+$ T cells in the livers of AAV-K^d-transduced mice than in those of mice transduced with the K^d-D227K vector, both on d7 ($9.97x10^4±2.1x10^4$ v/s $2.5x10^4±1.8x10^4$, p=0.0016) and d10 ($1.8x10^5±0.27x10^5$ v/s $1.6x10^4±0.5x10^4$, p<0.0001). n=3-4/group. (**B**) Activated $CD8^+$ T cells in the spleens of AAV-K^d treated mice outnumbered those in the spleens of mice receiving AAV-K^d-D227K on both d4 ($7.5x10^4±1.2x10^4$ v/s $2.1x10^4±6.8x10^3$) and d7 ($9.7x10±1.5x10^4$ v/s $4.5x10^4±1.0$ $x10^4$) post-inoculation. n=3-6/group. Statistical analysis for panels **A** and **B** was carried out using two-way ANOVA followed by Sidak's and Tukey's multiple comparisons tests. Box shows min to max, with a line at the mean. Data are described as mean±SEM.

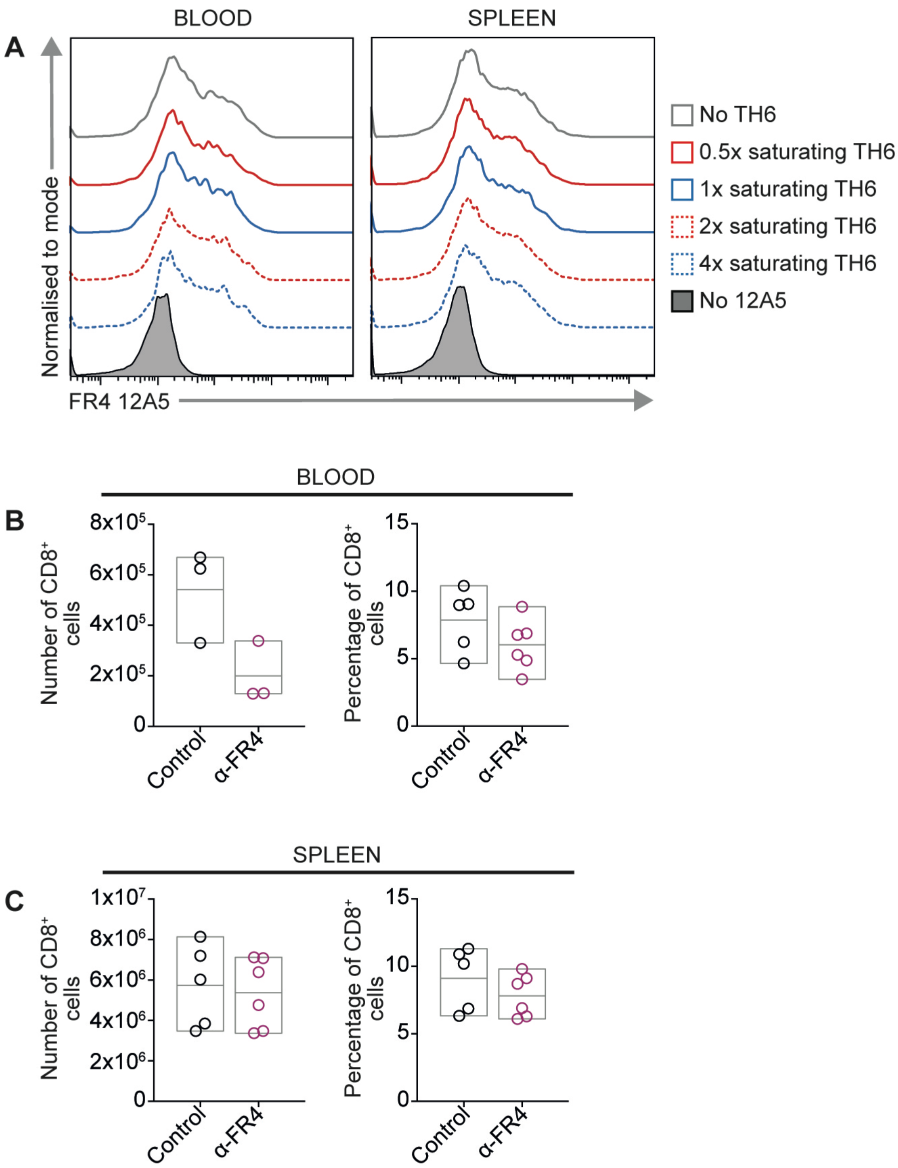

Supplementary Figure 6. Anti-FR4 antibody clone TH6 does not compete with 12A5 for binding to CD4$^+$ T cells. (**A**) In order to determine whether the depleting monoclonal antibody TH6 bound to the surface of FR4$^+$ T cells would compete with the detection antibody 12A5 for binding, we isolated 10^6 PBMC or splenocytes and stained them with both antibodies simultaneously. The concentration of 12A5 was kept constant, while concentrations of TH6 varied between 0.5x saturating and 4x saturating for 10^6 cells. The geometric mean fluorescence intensity for 12A5 staining gated on CD3$^+$CD4$^+$ T cells did not change appreciably as the concentration of TH6 increased, indicating that TH6 did not interfere with 12A5 binding. Neither the number nor the proportion of CD8$^+$ T cells in the peripheral blood (**B**) or spleen (**C**) of B10.BR mice was significantly altered following treatment with the anti-FR4 monoclonal antibody TH6. Boxes show min to max, with a line at the mean. Statistical analysis for **B-C** was perfomed using an unpaired T test.

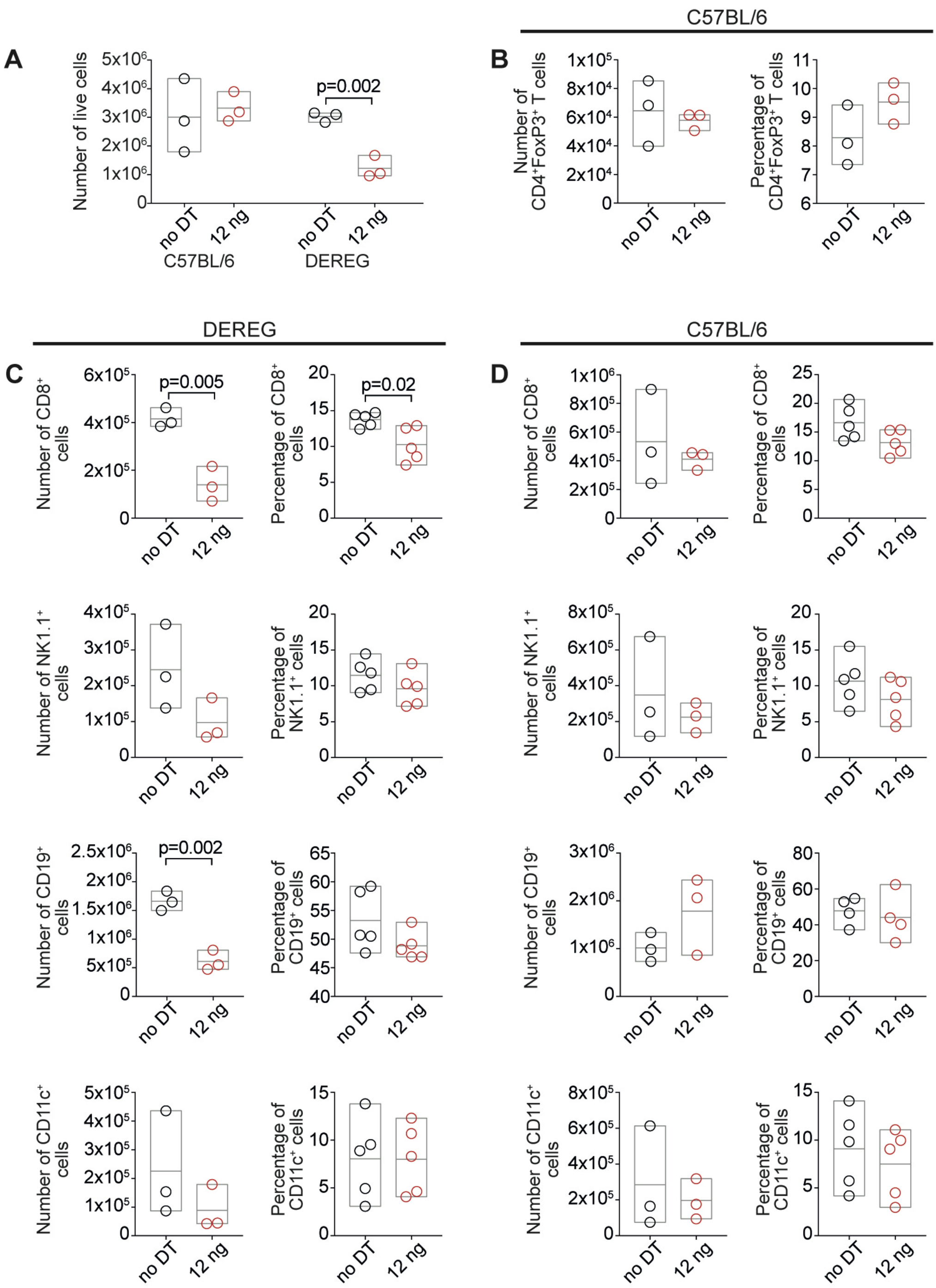

Supplementary Figure 7. Effect of Diphtheria Toxin treatment on cell subsets in C57BL/6 and DEREG peripheral blood. Peripheral blood samples from C57BL/6 or DEREG mice (n=3-5/group), either untreated, or injected with 12ng/g DT ip on 3 consecutive days were analysed by flow cytometry to determine the number and proportions of various leucocyte subsets. C57BL/6 samples were not affected by the DT treatment. In DEREG mice (**A**), there was an overall reduction in the total number of live cells recovered from peripheral blood ($1.23x10^6±2.26x10^5$ compared with $3.03x10^6±1.0x10^5$ in control mice, p=0.002). The absolute number of $CD8^+$ T cells fell from $4.15x10^5±2.39x10^4$ to $1.4x10^5±4.2x10^4$ (p=0.005, **D**) and this was mirrored by a decline in the fraction of $CD8^+$ T cells from 13.73±0.44% to 10.24±1.08%, p=0.02 (**E**). The number of $CD19^+$ cells in blood was reduced in DT-treated DEREG mice ($6.1x10^5±1.0x10^5$ v/s $1.66x10^6±9.77x10^4$ in controls, p=0.002, **L**) though there were no significant differences between the proportions of $CD19^+$ cells in these groups (**M**). Data are described as mean ± SEM, and unpaired T tests were used for all statistical analyses.

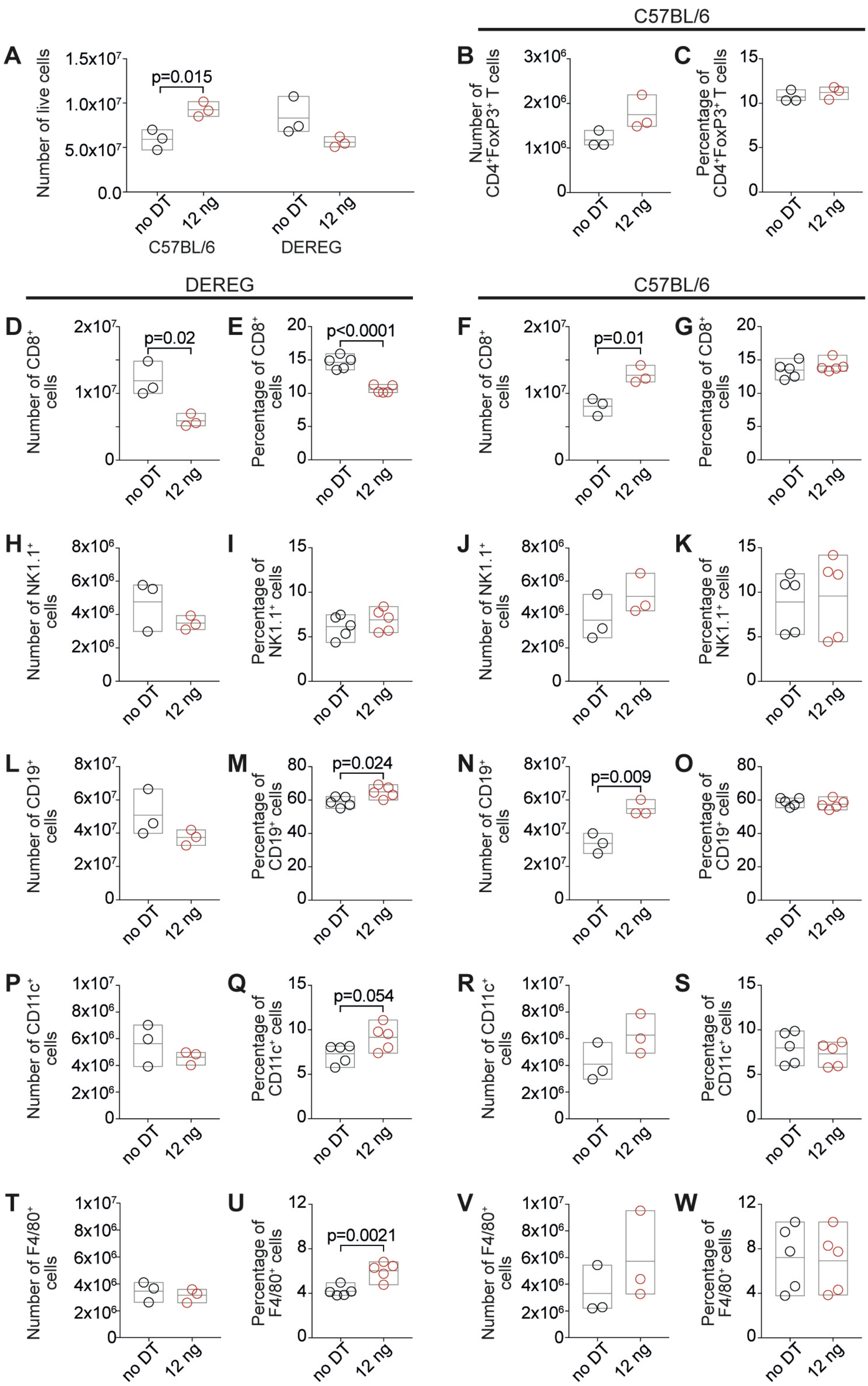

Supplementary Figure 8. Effect of Diphtheria Toxin treatment on cell subsets in C57BL/6 and DEREG spleen. Splenocyte samples from C57BL/6 or DEREG mice (n=3-5/group), either untreated, or injected with 12ng/g DT ip on 3 consecutive days were analysed by flow cytometry to determine the number and proportions of various leucocyte subsets. There was an overall increase in the number of live cells in DT-treated C57BL/6 mice ($9.27x10^7$±$4.85x10^6$ against $5.92x10^7$±$6.57x10^6$ in controls, p=0.015, **A**). The total number of cells recovered from DEREG spleens was not significantly altered by DT treatment (**A**). In C57BL/6 mice, neither the numbers (**B**) nor the proportion (**C**) of $CD4^+FoxP3^+$ T cells changed significantly in response to DT administration. The numbers of $CD8^+$ (**F**) and CD19+ (**N**) cells were increased by DT treatment, reflecting the overall increase in spleen cell numbers in DT-treated mice, but these changes were not accompanied by a corresponding increase in the percentage of these cell types (**G** and **O**). In DEREG spleen, the absolute number and proportion of $CD8^+$ cells was reduced by DT administration (**D** and **E**) while the proportion but not the number, of $CD19^+$ (**L**,**M**), $CD11c^+$ (**P**,**Q**), and $F4/80^+$ (**T**,**U**) cells increased. Boxes show min to max, with a line at the mean. Data are described as mean±SEM, and unpaired T tests were used for all statistical analyses.

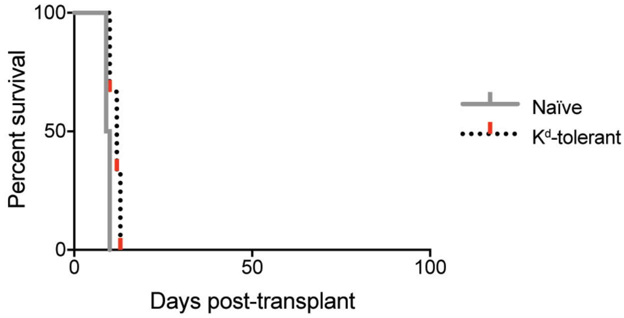

Supplementary Figure 9. Survival of Fully-mismatched Dba/2 (H-2^d) skin grafts is not prolonged in K^d-tolerant C57BL/6 recipients. To determine whether Tregs generated in response to either direct presentation of K^d or indirect presentation of K^d-derived peptides could mediate linked suppression of responses to other d-haplotype alloantigens, full haplotype mismatched Dba/2 skin grafts (H-2^d) were applied to K^d-tolerant C57BL/6 mice which had accepted B6.Kd skin grafts for more than 100 days following AAV-K^d inoculation, or to naïve C57BL/6 recipients. No survival prolongation was observed in K^d-tolerant mice.

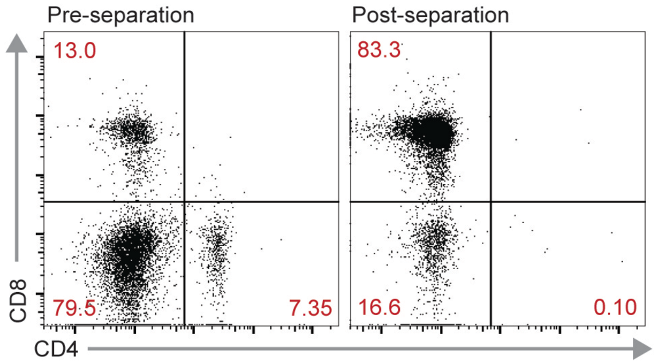

Supplementary Figure 10. CD8 enrichment prior to ELISpot assay. Prior to some ELISpot assays, CD8-enrichment of pooled, unfractionated splenocytes was carried out by negative bead selection using a CD8 α^{+} T Cell Isolation Kit and autoMACS Pro Separator (both, Miltenyi Biotec, Germany). CD8-enriched T cells from unprimed C57BL/6 mice and primed mice without AAV inoculation or transduced with either AAV-K^{d} or AAV-K^{d}-D227K (3 samples/group, each pooled from 3 mice/sample) were used as responder cells. Pre and post-separation, splenocytes were stained with antibodies against CD4 and CD8, and examined by flow cytometry. A representative dot-plot showing the enrichment of CD8^{+} and depletion of CD4^{+} cells is shown.